Asymmetric Addition of Ceramides but not Dihydroceramides Promotes Transbilayer (Flip-Flop) Lipid Motion in Membranes

F.-Xabier Contreras,* Gorka Basañez,* Alicia Alonso,* Andreas Herrmann,[†] and Félix M. Goñi*

*Unidad de Biofísica (Centro Mixto CSIC-UPV/EHU) and Departamento de Bioquímica, Universidad del País Vasco, 48080 Bilbao, Spain; and [†]Humboldt-Universität zu Berlin, Mathematisch-Naturwissenschaftliche Fakultät I, Institut für Biologie/Biophysik, D-10115 Berlin, Germany

ABSTRACT   Transbilayer lipid motion in membranes may be important in certain physiological events, such as ceramide signaling. In this study, the transbilayer redistribution of lipids induced either by ceramide addition or by enzymatic ceramide generation at one side of the membrane has been monitored using pyrene-labeled phospholipid analogs. When added in organic solution to preformed liposomes, egg ceramide induced transbilayer lipid motion in a dose-dependent way. Short-chain (C6 and C2) ceramides were less active than egg ceramide, whereas dihydroceramides or dioleoylglycerol were virtually inactive in promoting flip-flop. The same results (either positive or negative) were obtained when ceramides, dihydroceramides, or diacylglycerols were generated in situ through the action of a sphingomyelinase or of a phospholipase C. The phenomenon was dependent on the bilayer lipid composition, being faster in the presence of lipids that promote inverted phase formation, e.g., phosphatidylethanolamine and cholesterol; and, conversely, slower in the presence of lysophosphatidylcholine, which inhibits inverted phase formation. Transbilayer motion was almost undetectable in bilayers composed of pure phosphatidylcholine or pure sphingomyelin. The use of pyrene-phosphatidylserine allowed detection of flip-flop movement induced by egg ceramide in human red blood cell membranes at a rate comparable to that observed in model membranes. The data suggest that when one membrane leaflet becomes enriched in ceramides, they diffuse toward the other leaflet. This is counterbalanced by lipid movement in the opposite direction, so that net mass transfer between monolayers is avoided. These observations may be relevant to the physiological mechanism of transmembrane signaling via ceramides.

INTRODUCTION

Ceramides, or *N*-acyl sphingosines, constitute the basic structure of most sphingolipids, e.g., sphingomyelin or gangliosides. In the cell membrane, free ceramides occur mainly as intermediates in the metabolism of the more complex sphingolipids. However, ceramides have emerged in the last decade as important messengers in cell signaling, involved, among others, in processes of cell differentiation, growth suppression, and apoptosis (see (Pettus et al., 2002; Cremesti et al., 2002) for reviews). Although ceramides appear to exert many of their physiological effects through binding to specific sites in enzymes, other actions may take place through changes in the membrane physical properties (see review in Kolesnick et al., 2000). It is significant in this respect that ceramides have been shown to trigger vesicle efflux (Ruiz-Argüello et al., 1996; Siskind and Colombini, 2000; Montes et al., 2002), membrane fusion (Basañez et al., 1997; Ruiz-Argüello et al., 1998) and vesicle budding (Holopainen et al., 2000a), probably through the transient formation of non-bilayer intermediates (Kolesnick et al., 2000; Goñi and Alonso, 2000; Veiga et al., 1999). Moreover, ceramide in bilayers composed of phosphatidylcholine and/or sphingomyelin does not mix well with the phospholipids, giving rise to microdomains enriched in ceramide (Huang et al., 1996, 1999; Carrer and Maggio, 1999; Holopainen et al., 1997,

1998, 2000b, 2001; Fanani et al., 2002). This property of lateral segregation of ceramide-enriched lipid domains may explain that, at the cellular level, ceramide generated in rafts appears to induce their coalescence into large platforms, which would in turn serve as a site for oligomerization of cell surface receptors such as Fas and CD40 (Grassme et al., 2001, 2002) and the internalization of pathogenic bacteria, an idea suggested already by Holopainen et al. (2000c) and later experimentally demonstrated (Grassme et al., 2003; Gulbins et al., 2004).

A poorly understood aspect of ceramide signaling in cell physiology is that sphingomyelin (SM), perhaps the main source of ceramide in this context, is predominantly located in the outer monolayer of the plasma membrane, whereas ceramide receptor proteins are intracellular. Even if SM on the outer leaflet can be hydrolyzed by secreted forms of sphingomyelinase, the problem remains of how the resulting ceramide is translocated to the inner leaflet and becomes accessible to the intracellular proteins docking the plasma membrane. This issue has been addressed in recent work at this laboratory, and it has been shown that, both in model and cell membranes, ceramide generated in situ through the action of an externally added sphingomyelinase induced transbilayer lipid movements that presumably involved the translocation of ceramide together with other lipids (Contreras et al., 2003). This phenomenon was interpreted on the basis of another well-known ceramide property in membranes, i.e., its capacity to facilitate formation of

nonlamellar structures (Ruiz-Argüello et al., 1996; Veiga et al., 1999).

As a further step in the analysis of ceramide-induced flip-flop movements, we have tested the capacity of ceramide added externally to preexisting membranes (as opposed to in situ, enzyme-generated ceramide) to promote this kind of motion. Sphingomyelinase has a number of structural effects on vesicles, such as extensive aggregation (Ruiz-Argüello et al., 1996), that do not occur when ceramide is externally added; thus this work should be able to discern whether ceramide transbilayer transfer can occur in individual, nonaggregated membranes, or else it happens inseparably from vesicle aggregation. In our previous study (Contreras et al., 2003), we developed two novel methods to test lipid translocation; in this current article, we have applied yet another procedure, described by Müller et al. (2000) and based on the excimer-forming capacity of the fluorescent probe pyrene, incorporated into phosphatidylcholine or phosphatidylserine analogs. In addition to observing transbilayer lipid translocation in model and cell membranes induced by egg ceramide, whose N-acyl chain is predominantly palmitate (C16), we have tested short (C2 and C6) N-acyl chain ceramides, as well as the glycerolipid analog of ceramide, diacylglycerol. All three ceramides, and particularly the long-chain one, appear to be more active than diacylglycerol in promoting lipid flip-flop. The saturated dihydroceramides, which do not cause in cells the physiological effects of Δ^4 ceramides, also failed to induce transbilayer lipid motion.

MATERIALS AND METHODS

Materials

Sphingomyelinase (EC 3.1.4.12) from *Bacillus cereus* was obtained from Sigma (St. Louis, MO) and used in the presence of 2 mM o-phenanthroline to inhibit traces of contaminant phospholipase C activity. Previous studies showed that o-phenanthroline did not affect sphingomyelinase activity. Phosphatidylcholine-preferring phospholipase C (EC 3.1.4.1) from *B. cereus* was also purchased from Sigma. Egg SM, egg phosphatidylcholine, and egg phosphatidylethanolamine (PE) were obtained from Avanti Polar Lipids (Alabaster, AL). Cholesterol was from Sigma. Tetramethylrhodamine goat anti-mouse IgG (Rho-IgG) and N-(7-nitrobenzene-2-oxa-1,3-diazol-4-yl) phosphatidylethanolamine (NBD-PE) were supplied by Molecular Probes (Eugene, OR). 1-lauroyl-2-(1′-pyrenebutyroyl)-sn-glycero-3-phosphocoline (pyPC) and 1-lauroyl-2-(1′-pyrenebutyroyl)-sn-glycero-3-phosphoserine (pyPS) were synthesized as described in Müller et al. (2000). N-acetyl and N-hexanoyl ceramides, and their dihydroderivatives, as well as egg ceramide and dioleoylglycerol (DOG) were purchased from Avanti Polar Lipids. Dihydrosphingomyelin (dhSM) prepared by hydrogenation of egg sphingomyelin was a kind gift of Dr. J. P. Slotte (Åbo Akademi University, Turku, Finland).

Liposome preparation

Lipids were dissolved in chloroform/methanol, 2:1 (v/v), at the desired molar ratio. The lipid was deposited as a film on the wall of a glass test tube by solvent evaporation under nitrogen. Final traces of solvent were removed for 2 h in a vacuum chamber. The lipid film was suspended in the appropriate buffer

(10 mM HEPES, 200 mM NaCl, 10 mM CaCl$_2$, 2 mM MgCl$_2$, pH 6.5) by vortexing at room temperature to form multilamellar vesicles. The lipid suspensions were further processed through 10 cycles of freezing and thawing, followed by 10 passes through two filters (Nuclepore, Pleasanton, CA) of 0.1-μm pore diameter in an extruder at room temperature. The resulting vesicles had an average diameter of 120–150 nm, depending on lipid composition, according to quasielastic light-scattering measurements performed with a Malvern Zetasizer 4 instrument (Malvern Instruments, Malvern, UK). Chemical analysis of the extruded vesicles showed that the extrusion procedure did not modify their compositions. Liposomes (large unilamellar vesicles (LUVs)) were kept on ice and used immediately after preparation.

Erythrocyte ghosts

Ghost membranes were obtained from fresh human blood donated by healthy volunteers, as described in Fussle et al. (1981)

Asymmetric incorporation of pyPC or pyPS

To label vesicles only on the outer monolayer, an appropriate amount of pyPC or pyPS dissolved in chloroform/methanol was transferred into a glass tube and the solvent was evaporated under nitrogen. After solubilizing the analog in a small volume of ethanol, an aliquot (5 mol % of total lipid concentration) was added to the liposome suspension, and after vortex mixing, the system was left to equilibrate for 15 min at 37°C. Fluorescence measurements were performed with an Aminco-Bowman (Urbana, IL) spectrofluorometer series 2 using 1-ml quartz cuvettes with continuous stirring. Excitation wavelength was 344 nm. Emission wavelengths were 395 nm for monomers, and 465 nm for excimers. The incorporation of pyPC or pyPS into the outer membrane leaflet was followed by measuring the increase of the monomer/excimer ratio at 395 nm and 465 nm, respectively, as a function of time. Erythrocyte ghosts were labeled with pyPS in the same way as LUVs (Müller et al., 2000).

Ceramide and DOG preparation

Lipids in organic solvent were dried under nitrogen, and the final traces of solvent were removed for 1 h in a vacuum chamber. The dry lipids were resuspended in a small volume of ethanol or methanol for ceramides and DOG, respectively. The desired amount of ceramide or DOG was added, at 10 mol % of the final lipid concentration in all cases.

Ceramide and DOG incorporation into liposomal membranes

The extent of ceramide or DOG incorporation into liposomal membranes was estimated as follows. Multilamellar vesicles (MLVs) of SM/PE/Ch (2:1:1 mol ratio) were prepared by hydrating the dry lipid mixture in 10 mM HEPES, 200 mM NaCl, 10 mM CaCl$_2$, 2 mM MgCl$_2$, and pH 6.5 at room temperature, with vortex mixing. To 1 ml MLV suspension (300 μM total lipid), ceramide (or DOG) was added, at 30 μM final concentration in 2 μl ethanol (methanol for DOG). The mixture was incubated at 37°C, for 10 or 30 min. After incubation, the MLV suspensions were spun down in an Eppendorf (Hamburg, Germany) centrifuge at 14,000 × g for 5 min. This procedure achieved sedimentation of 100% of the lipid phosphorous when MLVs were processed in the absence of added ceramide or DOG. After centrifugation, pellets and supernatant were separately extracted with chloroform/methanol (2:1, v/v) and the lipids separated by thin-layer chromatography on 20-cm silica gel G plates. Mixtures containing DOG were separated with isopropyl ether/acetic acid (96:4, v/v) and the plates stained with Coomassie blue. Mixtures containing ceramide or dihydroceramide were separated with a two-solvent system: chloroform/methanol/

water (60:30:5 by volume) for the first 10 cm, and, after drying, petroleum ether/ethyl ether/acetic acid (60:40:1 by volume) for the whole length of the plate. Ceramide plates were stained by charring after 5% sulphuric acid treatment. Quantification was achieved by comparing the ceramide (or DOG) spots from pellet or supernatant with spots containing known amounts of each lipid, using a Bio-Rad (Hercules, CA) GS-800 densitometer. Note that, to facilitate separation between bound and unbound ceramide (or DOG), MLVs were used in this experiment, instead of the LUVs used in other measurements throughout this study. This means that the available surface of lipid bilayer accessible to ceramide or DOG was in this assay smaller than in the transbilayer lipid motion assays. Thus, the amounts of bound ceramide or DOG measured with this procedure represent actually the lower limits of binding under the regular experimental conditions.

Transbilayer lipid movement of pyrene-phospholipids in the presence of different lipids

The rate of transbilayer lipid diffusion (flip-flop) was measured using a method described by Müller et al. (2000). This method is based on the asymmetric incorporation of the pyrene probe pyPC or pyPS in the outer leaflet and the subsequent ''dilution'' of the probe as a result of transbilayer redistribution, leading to a decrease of excimer concentration. The probe stock solution was made in ethanol. All the experiments were performed at 37°C; lipid concentration was 300 μM for LUVs, to which 15 μM pyPC or pyPS was added. This results in the probe partitioning only into the outer monolayer. Sphingomyelinase was used at 1.6 U/ml. The final concentration of the different ceramides and DOG in buffer was 30 μM. Fluorescence intensities of excimers at 465 nm (I_E) and monomers at 395 nm (I_M) were taken from the spectra at various times. When flip-flop occurs, there is a reduction in the excimer-monomer ratio because of the dilution of the probe from one to both monolayers. The observed I_E/I_M was used to calculate the extent of flip-flop following the procedure of Müller et al. (2000). The dependence of I_E/I_M on the fraction of probe that had undergone transbilayer diffusion was calculated from a calibration curve as a function of the mole percent pyrene. The details of this calculation have been described (Müller et al., 2000). I_E/I_M of pyrene-phospholipid immediately after incorporation into the outer leaflet of vesicles was set to 1. Transbilayer lipid movement was monitored at an Aminco-Bowman spectrofluorometer series 2 as indicated above.

Transbilayer lipid movement demonstrated by fluorescence resonance energy transfer

This method was developed by Contreras et al. (2003), and is based on fluorescence resonance energy transfer between NBD and Rho. Rho was bound to an irrelevant IgG, whose large molecular weight (150,000) ensured that it could not penetrate the vesicles. LUVs were prepared as described above, including 0.6 mol % NBD-PE in the lipid mixture. To eliminate outer leaflet NBD-PE fluorescence, the vesicles were treated with 0.6 mM sodium dithionite that reduces NBD and quenches its fluorescence. Excess dithionite was removed passing the vesicle suspension through a Sephadex G-75 chromatography column (Amersham Biosciences, Uppsala, Sweden). For transbilayer lipid diffusion assays, LUVs (0.5 ml, 0.3 mM) containing NBD-PE only in the inner membrane leaflet were treated with 2 μl ceramide in ethanol, at 37°C, so that final ceramide concentration in the buffer was 30 μM. Aliquots (50 μl) were removed from the reaction mixture at regular intervals and mixed with 10 μl of Rho-IgG (2 mg/ml in 10 mM HEPES, 200 mM NaCl, 10 mM CaCl$_2$, 2 mM Mg Cl$_2$, pH 6.5 buffer) to a final volume of 0.5 ml. Fluorescence energy transfer was monitored at 37°C with an Aminco-Bowman spectrofluorometer series 2 in a continuously stirred cuvette. Excitation and emission wavelengths were 465 and 530 nm, respectively. A cutoff filter (515 nm) was used to reduce scattered light.

RESULTS

When pure pyPC (15 μM) was suspended in HEPES buffer the fluorescence emission spectrum was dominated by an excimer peak ($\lambda_{max} = 465$ nm) (Fig. 1 A, *solid line*), indicating organization of the analog in micelles. However, when the same amount of pyPC was incorporated asymmetrically into 0.3 mM LUV composed of SM/PE/Ch (2:1:1 mole ratio), the corresponding spectrum showed a high proportion of pyrene monomers ($\lambda_{max} = 395$ nm) (Fig. 1 A, *broken line*). Monomers occur as a result of dilution of pyPC in nonlabeled lipids (Galla and Hartmann, 1980; Müller et al., 2000; Somerharju, 2002). A decrease in the I_E/I_M ratio of fluorescence intensities corresponding respectively to excimer and monomer
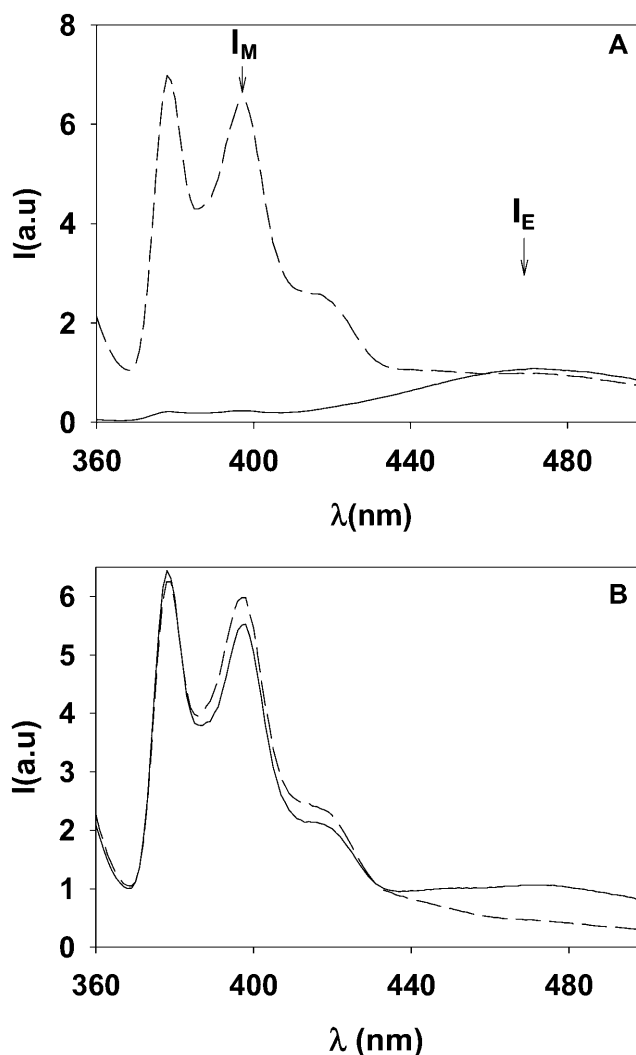

FIGURE 1 Fluorescence emission spectra of pyPC. (A) Solid line, 30 μM pyPC in HEPES buffer. Broken line, 15 μM pyPC incorporated asymmetrically (outer leaflet) into LUV (SM/PE/Ch, 2:1:1 mol ratio, 300 μM). (B) Solid line, pyPC (15 μM) incorporated asymmetrically into the outer monolayer of LUV (300 μM). *Broken line*, pyPC (15 μM) incorporated symmetrically into both monolayers of LUV (300 μM). See Methods for the spectral parameters.

emission was also observed when pyPC, originally present only in the outer monolayer of LUVs, became diluted into both monolayers. This is seen in Fig. 1 *B*: the solid line corresponds to a LUV preparation containing pyPC only in the outer monolayer, as indicated in the Methods section. The broken line corresponds to the spectrum of the same amount of pyPC mixed in organic solvent with the other lipids before liposome preparation, so that in the latter case the probe was symmetrically distributed in both monolayers. When pyPS was used instead of pyPC, spectra were almost identical to those in Fig. 1 (data not shown).

The proportion of monomers and excimers did not vary linearly with pyPC concentration in the bilayers. This is shown in Fig. 2 *A*, in which I_E and I_M are plotted as a function

of pyPC concentration in bilayers containing the probe in both leaflets, i.e., prepared by mixing the probe with the main lipids in organic solvent before vesicle preparation. Ideally one should obtain for the diluted (symmetrically distributed) probe a low I_E/I_M, high intensity values in absolute terms, and low probe concentration. As a compromise between those parameters, we settled on a 5 mol % (19:1 lipid/probe mole ratio) pyPC concentration in the bilayers for our further experiments.

The measured ratio I_E/I_M of pyPC in liposomal membranes corresponds to the excimer and monomer intensities of analogs in both leaflets, outer (I_E^o, I_M^o) and inner (I_E^i, I_M^i):

$$\frac{I_E}{I_M} = \frac{I_E^o + I_E^i}{I_M^o + I_M^i}.$$

To relate the observed I_E/I_M to the degree of pyPC distribution q between the leaflets,

$$q \equiv \frac{C_i}{C_i + C_o},$$

where C_i and C_o are the probe concentrations in the inner and outer monolayers, respectively. The data in Fig. 2 *A* can be used to construct a calibration curve, shown in Fig. 2 *B*. This curve is the basis for the q values given in Figs. 3–8, and in Table 1. For more details on the construction of the calibration curve, see Müller et al. (2000). A calibration curve (not shown) was similarly constructed for pyPS and used in the studies described in Figs. 9 and 10.

The binding of ceramides and DOG to liposome suspensions was estimated as indicated under Materials and Methods, by adding ceramides (or DOG) in organic solvent to preformed vesicles and then separating by centrifugation the bound and unbound fractions after incubation at 37°C. For C2-ceramide, the bound (pellet) fraction was 68.5 ± 2.4% after 10 min, and 66.7 ± 3.0% after 30 min incubation (average ± SD, $n = 3$). Simon and Gear (1998) found ≈80% binding under similar conditions. The fact that a significant fraction of C2-ceramide remains in the aqueous phase is in agreement with the idea that this short-chain ceramide behaves as a soluble amphiphile (Simon and Gear, 1998; J. Sot, unpublished observations). For egg ceramide, dihydroceramide, and DOG, the bound (pellet) fraction was >98% (average of three measurements) after 10 or 30 min incubation. Control experiments in which egg ceramides or DOG were centrifuged in the absence of vesicles showed that under these conditions, 100% of the ceramide or DOG floated and was recovered on top of the supernatant.

Ceramide-induced flip-flop movement of lipids is shown in Fig. 3. Curve *D* corresponds to the control experiment, with no additions. Curve *B* is a further control, to which 2 μl ethanol were added. When egg ceramide was added (in 2 μl ethanol) to a final 10 mol % concentration in the bilayer, an increase in q was detected (*curve A*), indicative of trans-bilayer lipid motion. When ceramide was generated in situ
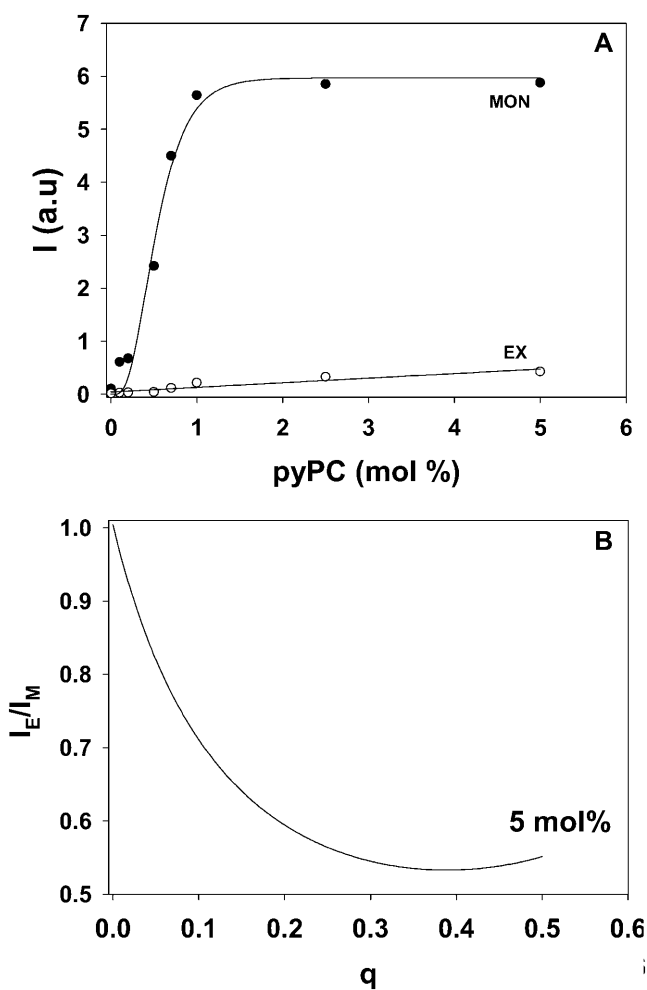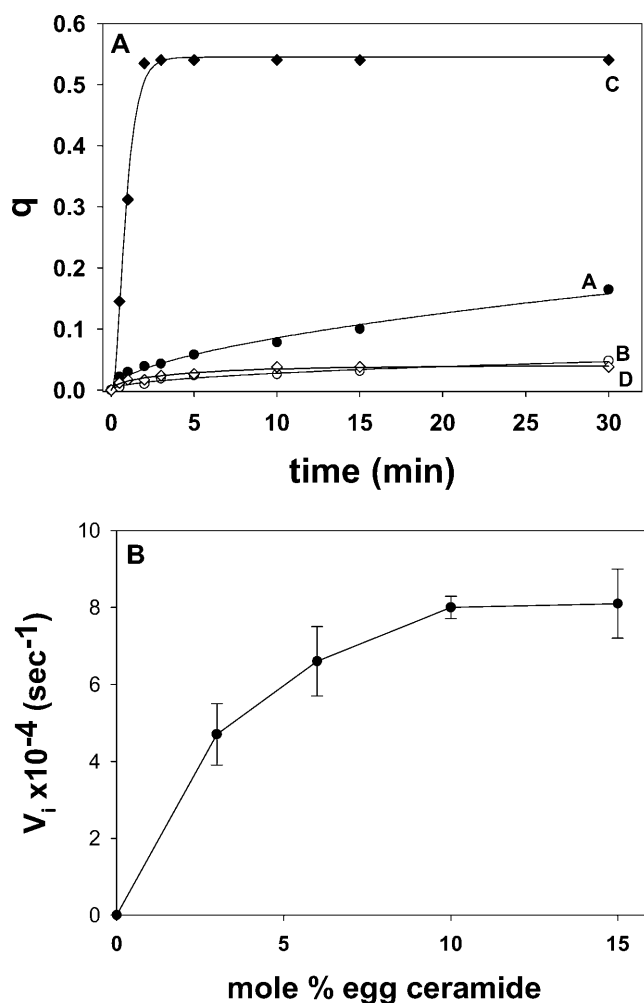
FIGURE 2 Fluorescence emission of pyPC in SM/PE/Ch LUV. (*A*) Intensities of monomers (○) measured at 395 nm and of excimers (●) measured at 465 nm as a function of pyPC concentration symmetrically incorporated in the bilayer. (*B*) The ratio I_E/I_M for different transbilayer distributions q in liposomal membranes containing 5 mol % pyPC. I_E and I_M, respectively, are the sum of the corresponding values in the inner (*i*) and outer (*o*) leaflet, ($I_E^i + I_E^o$) and ($I_M^i + I_M^o$), which were obtained from the experimental data in Fig. 3. See Müller et al. (2000) for details. I_E/I_M was set to 1 at $q = 0$.

FIGURE 3 Ceramide-induced transbilayer movement of pyPC in LUVs composed of SM/PE/Ch. The original lipid concentration was 300 μM. (A) The following additions were made to 1 ml of the LUV suspension at time zero: 30 μM (final concentration in buffer) egg ceramide in 2 μl ethanol (curve A), 2 μl ethanol (curve B), 1.6 U sphingomyelinase (curve C), and none (curve D). The data have been fitted to monoexponential curves of the form $y = a\,(1 - e^{-bx})^c$. (B) Dose-dependent effect of egg ceramide. Initial velocities (V_i) of transfer were measured from curves such as curve A in panel A. Average values $\pm$ SD ($n = 3$).

by adding sphingomyelinase (1.6 U/ml) to the liposome suspension (curve C), transbilayer motion was much faster, and q reached the theoretical upper value of $\sim$0.5 in 2–3 min. Under our conditions, sphingomyelinase cleaves $\sim$15% of the SM in the LUV to ceramide in the first 5 min (Contreras et al., 2003), thus the higher rate and amplitude of curve C with respect to curve A are not due to a higher amount of ceramide in C, but perhaps to a higher local concentration in ceramide-rich spots around the enzyme molecules. The data in Fig. 3 A correspond to single representative experiments. Average initial rates and q values after 30 min for 3–4 independent measurements have been summarized in Table 1. Egg ceramide effect on transbilayer motion was dose-dependent, as seen in Fig. 3 B.

In a previous study (Contreras et al., 2003), we demonstrated flip-flop movements of lipids using methods other than the pyrene-based procedure used in our current investigation. One of those methods is based on the fluorescence resonance energy transfer from NBD-PE to an IgG-bound rhodamine (Rho-IgG). NBD fluorescence in the bilayers is not modified by addition of ceramide (data not shown). Initially, NBD-PE is located only in the inner monolayer of the vesicles, and Rho-IgG is in the outside aqueous medium, so that energy transfer cannot occur. However, when NBD-PE flops to the outside monolayer, fluorescence resonance energy transfer to Rho-IgG occurs whenever a Rho-IgG molecule reaches the vesicle surface. A detailed description of representative experiments can be found in Contreras et al. (2003). Fig. 4 depicts in a comparative way transbilayer motion induced by egg ceramide and detected with either the pyPC method or the fluorescence energy transfer procedure. The fact that flip-flop is detected using two such different procedures confirms the observation that egg ceramide is indeed causing transbilayer lipid transfer.

The effect of short-chain ceramides can be seen in Fig. 5 and Table 1. Both C2- and C6-ceramide (suspended in buffer) induced flip-flop at initial rates similar to long-chain (egg) ceramide; however, q values after 30 min were smaller for the short-chain analogs (Fig. 5 A). The saturated analogs C2-dihydroceramide (Fig. 5 B, curve C) and C6-dihydroceramide (curve D) were much less effective than their unsaturated counterparts (curves A and B) in inducing transbilayer motion. When dioleoylglycerol (DOG) in methanolic solution was used instead of ceramide, no effect was seen (Table 1). A mixture of egg ceramide and DOG had the same effect as ceramide alone (Table 1). DOG is a very hydrophobic molecule that partitions readily into the lipid bilayer (see above); thus the lack of effect of DOG cannot be attributed to a failed incorporation into the membrane.

The inability of dihydroceramides or diacylglycerols to promote flip-flop motion was confirmed in experiments in which those lipids were enzymatically generated from their precursors dhSM or PE, respectively. In Fig. 6 A, the effects of sphingomyelinase on liposomes containing either SM or dhSM are compared. Under our conditions, the enzyme was equally active on SM and on dhSM: initial rates were, respectively, 54 $\pm$ 6.8 nmol SM min^{-1} and 49 $\pm$ 5.2 nmol dhSM min^{-1} ($n = 3$). Kuikka et al. (2001) had found that, under certain conditions, the enzyme may hydrolyze dhSM even more readily than SM. However dihydroceramide derived from dhSM was far less active than Δ^4-ceramide in promoting pyPC transbilayer motion (compare curves A and B in Fig. 6 A). A similar experiment was performed with bacterial phosphatidylcholine-preferring phospholipase C that is active on egg PE, yielding diacylglycerol. As shown in Fig. 6 B, PE was indeed hydrolyzed under our conditions, but no significant rate of flip-flop was observed.

In our recent study on sphingomyelinase-promoted transbilayer lipid motion (Contreras et al., 2003), it was suggested

TABLE 1 Transbilayer diffusion of pyrenyl-phospholipids induced by ceramide; a summary of results derived from experiments as shown in Figs. 3–9

Lipid composition	Probe	Additions	Initial rate $\times 10^4$ (s^{-1})	q_{30}
SM/PE/Ch (2:1:1)	pyPC	None	0.8 ± 0.002	0.05 ± 0.016
SM/PE/Ch (2:1:1)	pyPC	2 μl methanol	0.8 ± 0.08	0.04 ± 0.008
SM/PE/Ch (2:1:1)	pyPC	2 μl ethanol	0.8 ± 0.002	0.05 ± 0.006
SM/PE/Ch (2:1:1)	pyPC	10% egg ceramide*	3.7 ± 0.09	0.16 ± 0.018
SM/PE/Ch (2:1:1)	pyPC	10% C$_6$ ceramide*	4.0 ± 0.23	0.11 ± 0.013
SM/PE/Ch (2:1:1)	pyPC	10% C$_2$ ceramide*	4.0 ± 0.14	0.11 ± 0.018
SM/PE/Ch (2:1:1)	pyPC	1.6 U/ml SMase[†]	40.0 ± 2.8	0.54 ± 0.02
dhSM/PE/Ch (2:1:1)	pyPC	1.6 U/ml SMase[†]	5.0 ± 0.32	0.1 ± 0.03
SM/PE/Ch (2:1:1)	pyPC	10% DOG[‡]	0.8 ± 0.02	0.04 ± 0.003
SM/PE/Ch (2:1:1)	pyPC	10% egg ceramide + 10% DOG*[‡]	4.0 ± 0.07	0.16 ± 0.003
PC/PE/Ch (2:1:1)	pyPC	1.6 U/ml SMase[†]	0.8 ± 0.04	0.04 ± 0.01
SM (100%)	pyPC	None	0.8 ± 0.01	0.01 ± 0.009
SM (100%)	pyPC	10% egg ceramide*	0.8 ± 0.003	0.01 ± 0.005
SM/Ch (2:1)	pyPC	None	0.8 ± 0.03	0.01 ± 0.005
SM/Ch (2:1)	pyPC	10% egg ceramide*	0.9 ± 0.33	0.04 ± 0.004
SM/PE (2:1)	pyPC	None	0.8 ± 0.004	0.02 ± 0.008
SM/PE (2:1)	pyPC	10% egg ceramide*	0.8 ± 0.02	0.02 ± 0.005
PC (100%)	pyPC	None	0.8 ± 0.002	0.02 ± 0.01
PC (100%)	pyPC	10% egg ceramide*	0.8 ± 0.005	0.03 ± 0.006
SM/lysoPC/Ch (2:1:1)	pyPC	10% egg ceramide*	3.1 ± 0.80	0.05 ± 0.004
SM/PE/Ch/egg cer (2:1:1:0.4)	pyPC	10% egg ceramide*	17.3 ± 0.01	0.09 ± 0.02
Erythrocyte extract	pyPC	None	1.0 ± 0.02	0.03 ± 0.01
Erythrocyte extract	pyPC	2 μl ethanol	1.7 ± 0.01	0.04 ± 0.008
Erythrocyte extract	pyPC	10% egg ceramide*	6.3 ± 0.12	0.26 ± 0.03
Erythrocyte extract	pyPC	1.6 U/ml Smase[†§]	2.8 ± 0.45	0.26 ± 0.02
SM/PE/Ch (2:1:1)	pyPS	10% egg ceramide*	6.8 ± 0.35	0.33 ± 0.002
SM/PE/Ch (2:1:1)	pyPS	2 μl ethanol	1.2 ± 0.03	0.03 ± 0.03
Human RBC ghosts	pyPS	10% egg ceramide*	8.0 ± 0.07	0.14 ± 0.002
Human RBC ghosts	pyPS	2 μl ethanol	2.4 ± 0.02	0.03 ± 0.002

''Initial rate'' corresponds to the initial change in q over time. ''q_{30}'' is the value of q 30 min after ceramide addition. Average values $\pm$ SEM ($n = 3$).
*Added in 2 μl ethanol to 1 ml liposome suspension.
[†]Added in 32 μl buffer to 1 ml liposome suspension.
[‡]Added in 2 μl methanol to 1 ml liposome suspension.
[§]In this case, the initial rate was not the maximum rate; see Fig.8 and text.

that enzyme-generated ceramide induced the transient formation of nonlamellar structures, and that the latter caused the partial loss of asymmetry in the transbilayer lipid distribution. This suggestion was based on our previous observations of nonlamellar components (as detected by ^{31}P-NMR) in SM/PE/Ch liposomes treated with sphingomyelinase (Ruiz-Argüello et al., 1996), and our calorimetric observations of ceramides facilitating the lamellar-to-inverted hexagonal transition in phosphatidylethanolamine (Veiga et al., 1999). This suggestion has been tested with the pyPC system, by varying the LUV bilayer composition, and the results are shown in Fig. 7 and Table 1. It was found that the ceramide effects observed with SM/PE/Ch bilayers (*curve A*) were virtually abolished when either PE, or Ch, or both (curves *B–D*) were missing in the bilayer composition. Although structural studies for SM/PE or SM/Ch mixtures are not available, we observed that the PC/PE/Ch mixtures could undergo lamellar-to-nonlamellar transitions much more easily than PC/PE or PC/Ch binary compositions (Nieva et al., 1995), so it is likely that the same is true of SM-based

bilayers. In addition, the presence of lyso PC, a lipid known to stabilize the lamellar phase against formation of inverted nonlamellar phases, markedly inhibits flip-flop motion (*curve E*). Thus the data in Fig. 7 support the hypothesis that ceramide induces transbilayer lipid motion through facilitation of (transient) nonlamellar intermediates in the membrane.

In addition to transbilayer lipid motion (Contreras et al., 2003), sphingomyelinase action on LUVs containing SM causes vesicle aggregation (Ruiz-Argüello et al., 1996), and, under certain conditions (Ruiz-Argüello et al., 1998), perhaps fusion. Thus it is important to discern whether or not transbilayer lipid diffusion occurs associated with the other phenomena caused by the enzyme. The experiments in which flip-flop is induced by ceramide (Fig. 3) provide a good demonstration that transbilayer lipid motion occurs independently of vesicle aggregation. In fact, light-scattering measurements of LUVs before and after egg ceramide addition did not reveal any ceramide-dependent increase in size, apart from a small (<10%), fast ($t_{1/2} < 30$ s) increase in
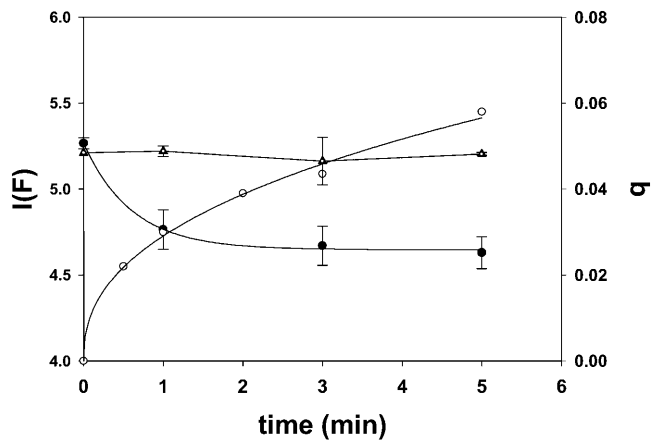
FIGURE 4 Egg ceramide-induced transbilayer lipid transfer demonstrated in LUVs composed of SM/PE/Ch, using two different methods. (○) Pyrene-PC method, data replotted from curve *A*, Fig. 3 *A*. (●) Fluorescence resonance energy transfer method (Contreras et al., 2003) using NBD-PE and IgG-Rho. The data show the decrease in NBD fluorescence intensity. The corresponding data showing an increase in Rho fluorescence intensity are not shown, for simplicity. (▲) Time-course of NBD fluorescence intensity in the absence of egg ceramide. Vesicle and ceramide concentrations as in Fig. 3 *A*. Average values ± SD (*n* = 3).

scattering upon ceramide addition, which reports on the ceramide incorporation to the lipid bilayers; thus no aggregation occurred (data not shown). The same light-scattering data could be used to discard any significant breakdown of vesicles upon ceramide addition, confirming previous observations that vesicles containing up to 20 mol % ceramide were stable for days at 4°C (Ruiz-Argüello et al., 1998). In our case we prepared vesicles containing 10 mol % egg ceramide (SM/PE/Ch/ceramide, 2:1:1:0.44) in which ceramide had been added in organic solution to the lipid mixture before vesicle formation. These vesicles did not support by themselves any detectable transbilayer diffusion. However, when egg ceramide was added in ethanol to the aqueous vesicle suspension, pyPC flip-flop was immediately observed to occur at a high rate (Fig. 7, *curve F*, and Table 1), although the phenomenon leveled off at a rather early stage. Ceramide preexisting in the bilayer may accelerate the initial steps of the molecular arrangements, leading ultimately to flip-flop, and this would explain the high initial rate. In turn, the presence of ceramide in the inner monolayer may work against transbilayer ceramide diffusion and be responsible for the relative small extent of lipid motion under these conditions (compare *curves A* and *F* in Fig. 7).

Essentially, the same results observed with bilayers of defined lipid compositions were obtained when LUVs were made of a composition resembling that of a cell membrane, namely an erythrocyte lipid extract (note however that transbilayer lipid distribution in LUVs would be essentially symmetrical). As seen in Fig. 8 and Table 1, ceramide induced flip-flop motion either when added externally (*curve B*) or when generated in situ (*curve A*). As in the case of LUVs with
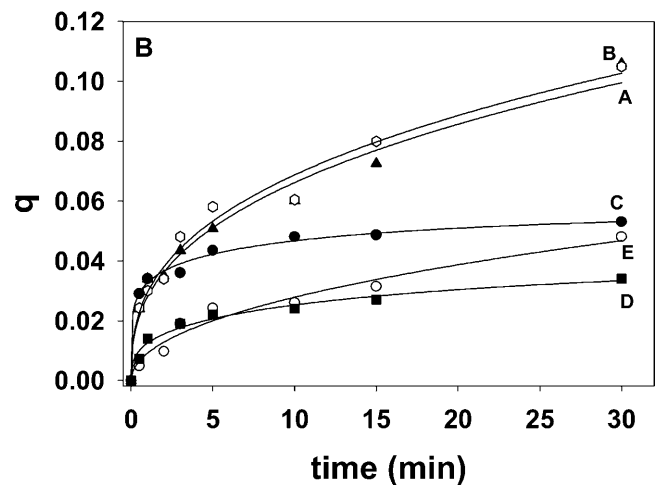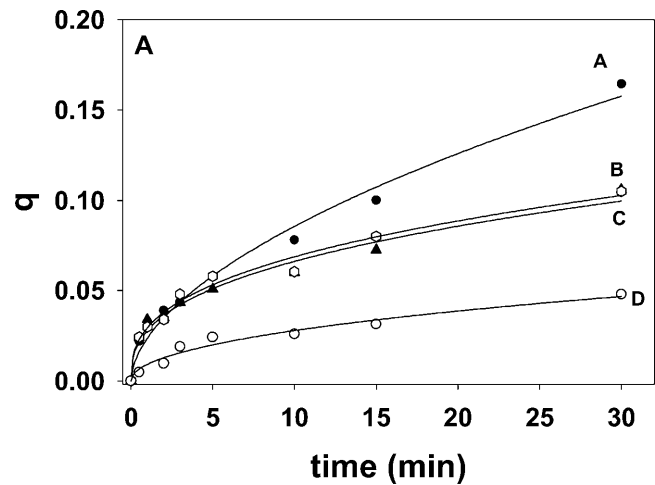

FIGURE 5 Transbilayer lipid motion induced by short-chain ceramides and dihydroceramides. LUV (300 μM) composed of SM/PE/Ch (2:1:1 mole ratio). (*A*) The following additions were made to 1 ml of the LUV suspension at time zero: 30 μM egg ceramide in 2 μl ethanol (curve *A*), 30 μM C6-ceramide in buffer (curve *B*), 30 μM C2-ceramide in buffer (curve *C*), and 2 μl ethanol (curve *D*). (*B*) Note the expanded ordinate scale: 30 μM C2-ceramide (curve *A*), 30 μM C6-ceramide (curve *B*), 30 μM C2-dihydroceramide (curve *C*), 30 μM c6-dihydroceramide (curve *D*), and 2 μl ethanol (curve *E*). Curve fitting as in Fig. 3 *A*.

a defined lipid composition, enzyme-generated ceramide induced faster and more extensive transbilayer lipid translocation than ceramide added in organic solvent. As seen in Fig. 8, *q* changes sigmoidally rather than hyperbolically in the presence of sphingomyelinase. This is due to the fact that the enzyme undergoes a lag phase with this (and other) lipid composition(s) (data not shown).

To further confirm and extend our previous observations, a number of experiments were repeated using a different pyrene probe, namely pyPS. The results were qualitatively similar, except that flip-flop appeared to be faster and more extensive when assayed with pyPS than with pyPC. An illustrative example is presented in Fig. 9, in which transbilayer diffusion induced by 10 mol % egg ceramide
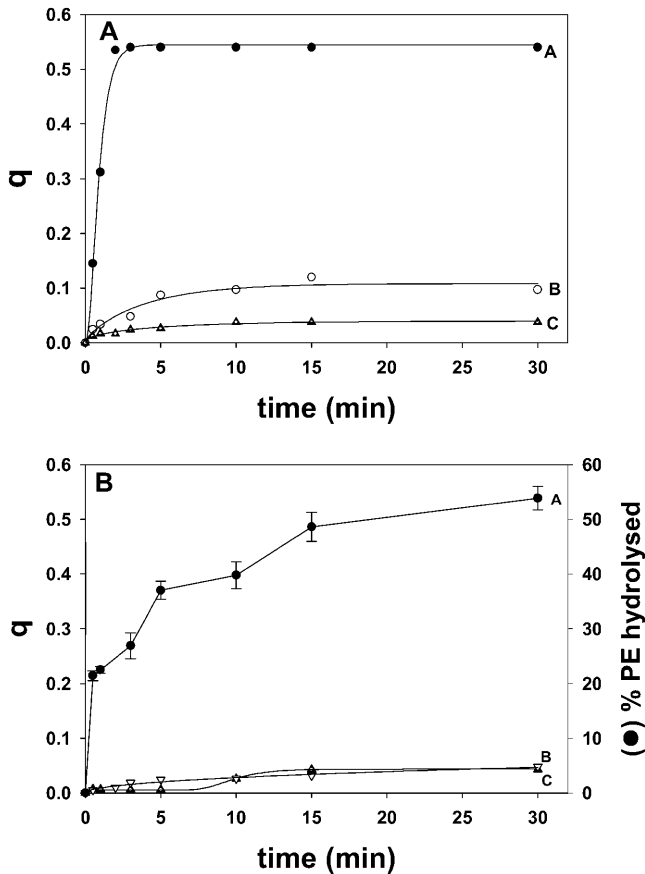
FIGURE 6 Transbilayer lipid motion induced by in situ enzymatically generated lipids in vesicles containing pyPC. (*A*) The enzyme was sphingomyelinase. Curve *A*, LUV composed of SM/PE/Ch (2:1:1 mol ratio); the enzyme yielded ceramide. Curve *B*, LUV composed of dhSM/PE/Ch (2:1:1 mol ratio); the enzyme yielded dihydroceramide. Curve *C*, LUV as in curve *B*, but no enzyme. (*B*) The enzyme was phospholipase C. LUV composed of SM/PE/Ch (2:1:1 mol ratio) Curve *A* (*right-hand axis*), PE hydrolysis. Average values ± SD (*n* = 3). Curve *B* (*left-hand axis*), transbilayer lipid motion in vesicles treated with phospholipase C. Curve *C* (*left-hand axis*) transbilayer lipid motion in vesicles with no enzyme added. When required, enzymes were added at time zero.

is followed through excimer dissociation of pyPS (*curve A*) or pyPC (*curve B*). The reasons why pyPS appears to be more responsive than pyPC are unclear at the moment. The higher signal provided by pyPS allowed us to apply our methods to the detection of ceramide-induced transbilayer lipid diffusion in a cell membrane, namely human erythrocyte ghosts. The results in Fig. 10 and Table 1 reveal that the initial rate and extent of transbilayer lipid transfer in a cell membrane are of the same order of magnitude as those in pure lipid bilayers.

DISCUSSION

Biomembranes are nonequilibrium structures, in which lipid asymmetry is maintained by active transbilayer lipid transport (Sillence et al., 2000; Traikia et al., 2002; Devaux and
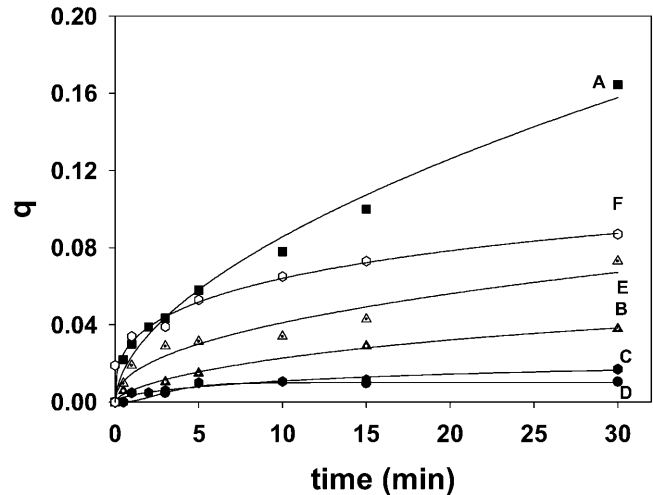

FIGURE 7 The influence of the bilayer lipid composition on ceramide-induced transbilayer pyPC motion; 30 μM egg ceramide was added to LUV suspensions (300 μM) of SM/PE/Ch, 2:1:1 mol ratio (*curve A*), SM/Ch, 2:1 mol ratio (*curve B*), SM/PE, 2:1 mol ratio (*curve C*), pure SM (*curve D*), SM/lysoPC/Ch, 2:1:1 mol ratio (*curve E*), and SM/PE/Ch/egg ceramide, 2:1:1:0.4 mol ratio (*curve F*). Data fitting as in Fig. 3 *A*.

Morris, 2004). Experimental tools to assess this kind of molecular motion have not been available until recently (Pomorski et al., 1996; Devaux et al., 2002). In our previous article (Contreras et al., 2003), we developed two novel methods of flip-flop assay, and in our current article we have applied a convenient procedure developed by Müller et al. (2000). It should be noted that, in our studies, the molecule reporting the motion is different from the one causing it. The
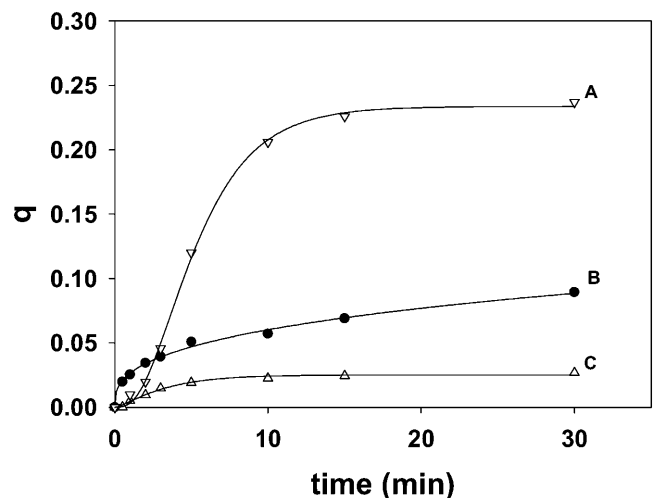

FIGURE 8 Transbilayer diffusion of pyPC in LUVs formed from an erythrocyte lipid extract. The original lipid concentration was 300 μM. The following additions were made to 1 ml LUV suspension at time zero: 1.6 U sphingomyelinase (*curve A*), 30 μM egg ceramide (*curve B*), and none (*curve C*). Data fitting as in Fig. 3. (*Curve A* was fitted to a sigmoidal curve.)
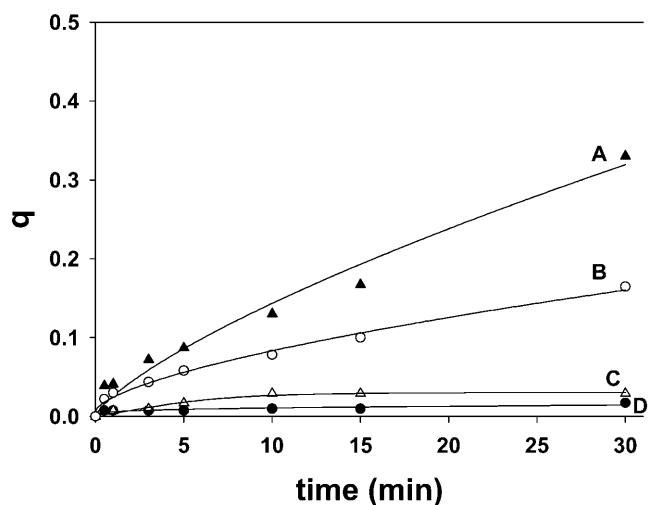
FIGURE 9 Ceramide-induced transbilayer movement of pyPC and pyPS in LUVs composed of SM/PE/Ch. Experimental details as in Fig. 3 *A*. (*Curve A*) 30 μM egg ceramide, bilayers containing 5 mol % pyPS. (*Curve B*) 30 μM egg ceramide, bilayers containing 5 mol % pyPC. (*Curve C*) 2 μl ethanol, bilayers containing pyPS. (*Curve D*) 2 μl ethanol, bilayers containing pyPC. Curve fitting as in Fig. 3 *A*.

latter is always a ceramide, either added to the preformed vesicle (this work) or generated in situ via a sphingomyelinase (Contreras et al., 2003). The reporter molecule instead is either a ganglioside ("neuraminidase method" (Contreras et al., 2003)), NBD-PE ("resonance energy transfer method" (Contreras et al., 2003) or Fig. 4 in this article), or a pyrene-derivatized phospholipid (this work). Depending on the approach, the reporter molecules were initially incorporated asymmetrically either in the outer (ganglioside, pyPC, pyPS) or the inner (NBD-PE) leaflet. When com-
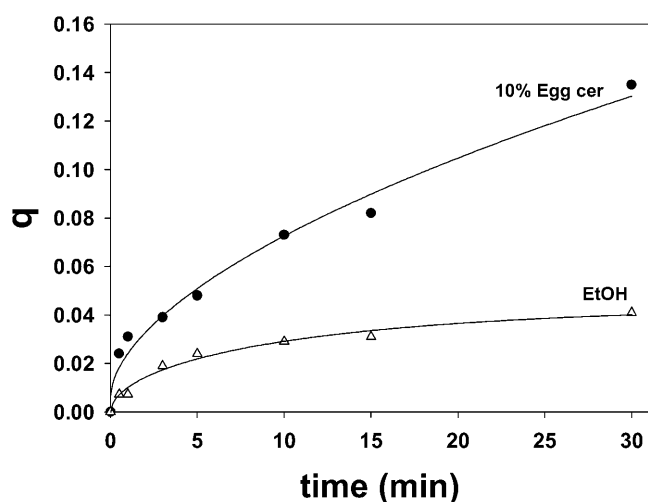

FIGURE 10 Flip-flop lipid motion in human red blood cell membrane ghosts labeled with pyPS. Membrane ghost suspension (1 ml) contained 300 μl lipid. Either 30 μM egg ceramide in 2 μl ethanol (●) or just 2 μl ethanol (△) were added at time zero. Curve fitting as in Fig. 3 *A*.

paring the results, inward and outward rates appear to be of the same order of magnitude. A simple interpretation of these observations is that there is a tendency toward mass conservation in each monolayer, so that transfer of lipids in one direction is compensated by the simultaneous transfer of (the same or) other lipids in the reciprocal direction. The opposite situation, namely the net transfer of mass (lipid molecules), would lead to untenable increases in lateral pressure, thus to bilayer collapse. Note that there may be net transfer of a given chemical species (e.g., ceramide) without significant net transfer of mass, if movement of a given lipid in one direction is compensated by a reciprocal transfer of a different lipid molecule.

However, although mass conservation may explain the reciprocal nature of transbilayer lipid motion, the question on the driving force still remains. In our previous article (Contreras et al., 2003), we suggested that it could be related to the capacity of ceramides to induce formation of non-lamellar inverted phases (Ruiz-Argüello et al., 1996, 1998; Veiga et al., 1999). The data in our current work support this hypothesis, in particular the observation that PE and Ch, which are known to facilitate formation of inverted phases (Nieva et al., 1995), also increase the rate and extent of transbilayer lipid transfer (Fig. 7). In contrast, the latter was not observed for lysoPC, which stabilizes the lamellar phase against the transition to inverted phases (Fig. 7, *curve E*). Moreover, short-chain ceramides (C2 and C6) appear to be less potent than C16-ceramide in facilitating the lamellar-to-inverted hexagonal transition of phospholipids (J. Sot and F. M. Goñi, unpublished data), and this would be in agreement with their lower ability to trigger flip-flop between monolayers (Fig. 5). Apart from, or in conjunction with, ceramide ability to induce inverted phase formation, a difference in lateral pressure between the two leaflets may be required for the induction of phospholipid translocation. When ceramide is added to the preformed vesicles, ceramide insertion will initially increase surface pressure in the outer monolayer. When ceramide formation is induced by sphingomyelinase, the reciprocal phenomenon will occur, and surface pressure will initially decrease in the outer monolayer as SM molecules are converted into ceramide (ceramide has a cross-sectional area of 40 Å^2 at 25 mN/m (Maggio et al., 1978), whereas SM has $\sim$55 Å^2 (Reiss-Husson, 1967)), so that a difference in lateral pressure will also occur in this case. No such difference exists when ceramides are incorporated in the initial liposome lipid mixture, and no lipid flip-flop is observed in that case.

The inability of dihydroceramides to induce flip-flop motion (Fig. 6 *A*) is worth noting, because dihydroceramides appear to lack many physiological effects of Δ^4-ceramides (Kolesnick et al., 2000). There are few comparative studies on the physical properties of unsaturated and dihydroceramides. Li et al. (2002), using nuclear magnetic resonance, observed that the lack of the *trans*-Δ^4 double bond leads to a conformational distortion of this part of the molecule, so

that the degree with which water molecules stabilize the H-bonds between the two OH groups of the sphingolipid is reduced in the saturated ceramide with respect to the Δ^4-ceramide. SM and dhSM have also significantly different physical properties, with dhSM increasing the stability and cohesion of membranes as compared to SM (Kuikka et al., 2001; Olilla and Slotte, 2002; Nyholm et al., 2003a,b).

It remains also unexplained why DOG, which becomes inserted in the bilayer and is more potent than ceramide in promoting the lamellar-hexagonal transition (Veiga et al., 1999), does not facilitate flip-flop motion (Fig. 6 B). Previous studies from this (Ruiz-Argüello et al., 1996, 1998) and other laboratories (Holopainen et al., 2002; Riske and Dobereiner, 2003) have described other instances in which ceramides and diacylglycerides, despite their structural similarities, perturb bilayers in very different ways.

When considering the mechanism of ceramide-induced transbilayer motion, and the forces behind it, an important fact is that changes in lipid asymmetry are often directly coupled to changes in vesicle morphology and vesicle transformation, including vesicle budding and fission (Dobereiner et al., 1993; Holopainen et al., 2000a), transformation of initially invaginated LUVs into long narrow tubular structures, or into spherical structures with one or more protrusions (Mui et al., 1995). Asymmetric generation of diacylglycerol through phospholipase C activity on unilamellar vesicles gives rise to major changes in bilayer architecture, including vesicle fusion, and ultimately vesicle collapse (Goñi and Alonso, 2000; Riske and Dobereiner, 2003). Vesicle aggregation (Ruiz-Argüello et al., 1996) and perhaps also fusion (Ruiz-Argüello et al., 1998; Basañez et al., 1997) occur as a result of enzymatic generation of ceramide in the outer monolayer. These substantial structural changes could in principle be related to the observed ceramide-induced transbilayer lipid motion, but, in fact, as mentioned in connection with Fig. 3 in the Results section, it does not appear to be the case, since addition of egg ceramide to LUVs in suspension under our conditions is not accompanied by significant changes in light scattering, which would occur if major structural changes, of the kind discussed above, were taking place. Obviously this does not preclude that, under the circumstances where those large morphological changes are taking place, transbilayer lipid motion might additionally occur.

An increasing number of physiological events are being associated with lipid flip-flop in the recent years. To mention but a few examples, lipid asymmetry is altered in physiological or pathological events such as phagocyte recognition, blood coagulation, or apoptosis (Bevers et al., 1999). Some of these phenomena may be catalyzed by a ''scramblase'' (Zhou et al., 1997; Frasch et al., 2004). An energy-independent protein activity has been described that catalyzes rather unspecific glycerophospholipid transbilayer motion in the endoplasmic reticulum (Buton et al., 1996; Bishop and Bell, 1985; Herrmann et al., 1990).

Pore-forming peptides induce phospholipid flip-flop in membranes (Fattal et al., 1994; Basañez et al., 2002), and the same is true of the proapoptotic protein Bax (Terrones et al., 2004; Epand et al., 2003). Insertion of the ''adenylate cyclase toxin'' from B. pertussis in lipid bilayers is also accompanied by transbilayer lipid transfer (Martín et al., 2004). Moreover, it has been suggested that the transmembrane domains of several integral proteins of the bacterial cytoplasmic membrane may facilitate phospholipid translocation (Kol et al., 2003). It is unclear at the moment whether these multifarious phenomena share common mechanisms of transbilayer lipid transfer; further research is required to clarify this point.

The possible physiological significance of the observations in this article should not be ignored. Kinnunen and Holopainen (2002) described that human serum low-density lipoprotein has a sphingomyelinase activity, and suggested a mechanistic link between elevated plasma levels of the lipoprotein, ceramide, apoptosis, and atherosclerosis. Also, over the past decade, a large number of direct targets for ceramide have been shown to act as mediators of ceramide signaling, e.g., kinase suppressor of Ras, ceramide-activated protein phosphatase, various protein kinase C isoforms, etc. (see Pettus et al., 2002; Cremesti et al., 2002; and Kolesnick et al., 2000, for reviews). However, these targets are intracellular. In turn, most of the sphingomyelin in the plasma membrane exists in the outer leaflet, perhaps in the form of rafts (Simons and Ikonen, 2000), and acid sphingomyelinase appears to be translocated onto the outer leaflet to perform the hydrolytic cleavage of SM (Grassme et al., 2001, 2002, 2003). Our data on model and cell membranes support the idea that ceramide, generated in the outer leaflet, will spontaneously distribute between both monolayers, thus becoming accessible to cytosolic protein targets that may (transiently) dock to the plasma membrane inner monolayer.

REFERENCES

Basañez, G., M. B. Ruiz-Argüello, A. Alonso, F. M. Goñi, G. Karlsson, and K. Edwards. 1997. Morphological changes induced by phospholipase C and by sphingomyelinase on large unilamellar vesicles: a cryo-transmission electron microscopy study of liposome fusion. *Biophys. J.* 72: 2630–2637.

Basañez, G., A. E. Shinnar, and J. Zimmerberg. 2002. Interaction of hagfish cathelicidin antimicrobial peptides with model lipid membranes. *FEBS Lett.* 532:115–120.

Bevers, E. M., P. Comfurius, D. W. C. Dekkers, and R. F. A. Zwaal. 1999. Lipid translocation across the plasma membrane of mammalian cells. *Biochim. Biophys. Acta.* 1439:317–330.

Bishop, W. R., and R. M. Bell. 1985. Assembly of the endoplasmic reticulum phospholipid bilayer: the phosphatidylcholine transporter. *Cell.* 42:51–60.

Buton, X., G. Morrot, P. Fellmann, and M. Seigneuret. 1996. Ultrafast glycerophospholipid-selective transbilayer motion mediated by a protein in the endoplasmic reticulum membrane. *J. Biol. Chem.* 271:6651–6657.

Carrer, D. C., and B. Maggio. 1999. Phase behavior and molecular interactions in mixtures of ceramide with dipalmitoylphosphatidylcholine. *J. Lipid Res.* 40:1978–1989.

Contreras, F. X., A. V. Villar, A. Alonso, R. N. Kolesnick, and F. M. Goñi. 2003. Sphingomyelinase activity causes transbilayer lipid translocation in model and cell membranes. *J. Biol. Chem.* 278:37169–37174.

Cremesti, A. E., F. M. Goñi, and R. N. Kolesnick. 2002. Role of sphingomyelinase and ceramide in modulating rafts: do biophysical properties determine biologic outcome? *FEBS Lett.* 531:47–53.

Devaux, P. F., and R. Morris. 2004. Transmembrane asymmetry and lateral domains in biological membranes. *Traffic.* 5:241–246.

Devaux, P. F., P. Fellmann, and P. Herve. 2002. Investigation on lipid asymmetry using lipid probes: comparison between spin-labeled lipids and fluorescent lipids. *Chem. Phys. Lipids.* 116:115–134.

Dobereiner, H. G., J. Kas, D. Noppl, I. Sprenger, and E. Sackmann. 1993. Budding and fission of vesicles. *Biophys. J.* 65:1396–1403.

Epand, R. F., J. C. Martinou, S. Montessuit, and R. M. Epand. 2003. Transbilayer lipid diffusion promoted by Bax: implications for apoptosis. *Biochemistry.* 42:14576–14582.

Fanani, M. L., S. Hartel, R. G. Oliveira, and B. Maggio. 2002. Bidirectional control of sphingomyelinase activity and surface topography in lipid monolayers. *Biophys. J.* 83:3416–3424.

Fattal, E., S. Nir, R. A. Parente, and F. C. Szoka. 1994. Pore-forming peptides induce rapid phospholipid flip-flop in membranes. *Biochemistry.* 33:6721–6731.

Frasch, S. C., P. M. Henson, K. Nagaosa, M. B. Fessler, N. Borregaard, and D. L. Bratton. 2004. Phospholipid flip-flop and phospholipid scramblase 1 (PLSCR1) co-localize to uropod rafts in formylated Met-Leu-Phe-stimulated neutrophils. *J. Biol. Chem.* 279:17625–17633.

Fussle, R., S. Bhakdi, A. Sziegoleit, J. Tranum-Jensen, T. Krans, and H. J. Wellensiek. 1981. On the mechanism of membrane damage by Staphylococcus aureus alpha-toxin. *J. Cell Biol.* 91:83–94.

Galla, H. J., and W. Hartmann. 1980. Excimer-forming lipids in membrane research. *Chem. Phys. Lipids.* 27:199–219.

Goñi, F. M., and A. Alonso. 2000. Membrane fusion induced by phospholipase C and sphingomyelinases. *Biosci. Rep.* 20:443–463.

Grassme, H., V. Jendrossek, J. Bock, A. Riehle, and E. Gulbins. 2002. Ceramide-rich membrane rafts mediate CD40 clustering. *J. Immunol.* 168:298–307.

Grassme, H., V. Jendrossek, A. Riehle, G. Von Kurthy, G. Berger, H. Schwartz, M. Weller, R. Kolesnick, and E. Gulbins. 2003. Host defense against Pseudomonas aeruginosa requires ceramide-rich membrane rafts. *Nat. Med.* 9:322–330.

Grassme, H., H. Schwartz, and E. Gulbins. 2001. Molecular mechanisms of ceramide-mediated CD95 clustering. *Biochem. Biophys. Res. Commun.* 284:1016–1030.

Gulbins, E., S. Dreschers, B. Wilker, and H. Grassme. 2004. Ceramide, membrane rafts and infections. *J. Mol. Med.* 82:357–363.

Herrmann, A., A. Zachowski, and P. F. Devaux. 1990. Protein-mediated phospholipid translocation in the endoplasmic reticulum with a low lipid specificity. *Biochemistry.* 29:2023–2027.

Holopainen, J. M., M. I. Angelova, and P. K. J. Kinnunen. 2000a. Vectorial budding of vesicles by asymmetrical enzymatic formation of ceramide in giant liposomes. *Biophys. J.* 78:830–838.

Holopainen, J. M., M. I. Angelova, T. Soderlund, and P. K. Kinnunen. 2002. Macroscopic consequences of the action of phospholipase C on giant unilamellar liposomes. *Biophys. J.* 83:932–943.

Holopainen, J. M., H. L. Brockman, R. E. Brown, and P. K. Kinnunen. 2001. Interfacial interactions of ceramide with dimyristoylphosphatidylcholine: impact of the N-acyl chain. *Biophys. J.* 80:765–775.

Holopainen, J. M., J. Y. Lehtonen, and P. K. Kinnunen. 1997. Lipid microdomains in dimyristoylphosphatidylcholine-ceramide liposomes. *Chem. Phys. Lipids.* 88:1–13.

Holopainen, J. M., J. Lemmich, F. Richter, O. G. Mouritsen, G. Rapp, and P. K. Kinnunen. 2000b. Dimyristoylphosphatidylcholine/C16:0-ceramide binary liposomes studied by differential scanning calorimetry and wide- and small-angle x-ray scattering. *Biophys. J.* 78:2459–2469.

Holopainen, J. M., O. P. Medina, A. J. Metso, and P. K. Kinnunen. 2000c. Sphingomyelinase activity associated with human plasma low density lipoprotein. *J. Biol. Chem.* 275:16484–16489.

Holopainen, J. M., M. Subramanian, and P. K. Kinnunen. 1998. Sphingomyelinase induces lipid microdomain formation in a fluid phosphatidylcholine/sphingomyelin membrane. *Biochemistry.* 37:17562–17570.

Huang, H. W., E. M. Goldberg, and R. Zidovetzki. 1999. Ceramides modulate protein kinase C activity and perturb the structure of phosphatidylcholine/phosphatidylserine bilayers. *Biophys. J.* 77:1489–1497.

Huang, H. W., E. M. Goldberg, and R. Zidovetzki. 1996. Ceramide induces structural defects into phosphatidylcholine bilayers and activates phospholipase A2. *Biochem. Biophys. Res. Commun.* 220:834–838.

Kinnunen, P. K., and J. M. Holopainen. 2002. Sphingomyelinase activity of LDL: a link between atherosclerosis, ceramide, and apoptosis? *Trends Cardiovasc. Med.* 12:37–42.

Kol, M. A., A. van Dalen, A. I. P. M. de Kroon, and B. de Kruijff. 2003. Translocation of phospholipids is facilitated by a subset of membrane-spanning proteins of the bacterial cytoplasmic membrane. *J. Biol. Chem.* 278:24586–24593.

Kolesnick, R. N., F. M. Goñi, and A. Alonso. 2000. Compartmentalization of ceramide signaling: physical foundations and biological effects. *J. Cell. Physiol.* 184:285–300.

Kuikka, M., B. Ramstedt, H. Ohvo-Rekila, J. Tuuf, and J. P. Slotte. 2001. Membrane properties of D-erythro-N-acyl sphingomyelins and their corresponding dihydro species. *Biophys. J.* 80:2327–2337.

Li, L., X. Tang, K. G. Taylor, D. B. DuPre, and M. C. Yappert. 2002. Conformational characterization of ceramides by nuclear magnetic resonance spectroscopy. *Biophys. J.* 82:2067–2080.

Maggio, B., F. A. Cumar, and R. Caputto. 1978. Surface behaviour of gangliosides and related glycosphingolipids. *Biochem. J.* 171:559–565.

Martín, C., M. A. Requero, J. Masin, I. Konopasek, F. M. Goñi, P. Sebo, and H. Ostolaza. 2004. Membrane restructuring by Bordetella pertussis adenylate cyclase toxin, a member of the RTX toxin family. *J. Bacteriol.* 186:3760–3765.

Montes, L. R., F. M. Goñi, and A. Alonso. 2002. Membrane restructuring via ceramide results in enhanced solute efflux. *J. Biol. Chem.* 277:11788–11794.

Mui, B. L., H. G. Dobereiner, T. D. Madden, and P. R. Cullis. 1995. Influence of transbilayer area asymmetry on the morphology of large unilamellar vesicles. *Biophys. J.* 69:930–941.

Müller, P., S. Schiller, T. Wieprecht, M. Dathe, and A. Herrmann. 2000. Continuous measurement of rapid transbilayer movement of a pyrene-labeled phospholipid analogue. *Chem. Phys. Lipids.* 106:89–99.

Nieva, J. L., A. Alonso, G. Basañez, F. M. Goñi, A. Gulik, R. Vargas, and V. Luzzati. 1995. Topological properties of two cubic phases of a phospholipid:cholesterol: diacylglycerol aqueous system and their possible implications in the phospholipase C-induced liposome fusion. *FEBS Lett.* 368:143–147.

Nyholm, T. K., M. Nylund, and J. P. Slotte. 2003a. A calorimetric study of binary mixtures of dihydrosphingomyelin and sterols, sphingomyelin, or phosphatidylcholine. *Biophys. J.* 84:3138–3146.

Nyholm, T., M. Nylund, A. Soderholm, and J. P. Slotte. 2003b. Properties of palmitoyl phosphatidylcholine, sphingomyelin, and dihydrosphingo-

myelin bilayer membranes as reported by different fluorescent reporter molecules. *Biophys. J.* 84:987–997.

Ollila, F., and J. P. Slotte. 2002. Partitioning of Triton X-100, deoxycholate and C(10)EO(8) into bilayers composed of native and hydrogenated egg yolk sphingomyelin. *Biochim. Biophys. Acta.* 1564:281–288.

Pettus, B. J., C. E. Chalfant, and Y. A. Hannun. 2002. Ceramide in apoptosis: an overview and current perspectives. *Biochim. Biophys. Acta.* 1585:114–125.

Pomorski, T., P. Muller, B. Zimmermann, K. Burger, P. F. Devaux, and A. Herrmann. 1996. Transbilayer movement of fluorescent and spin-labeled phospholipids in the plasma membrane of human fibroblasts: a quantitative approach. *J. Cell Sci.* 109:687–698.

Reiss-Husson, F. 1967. Structure of liquid-crystalline phases of different phospholipids, monoglycerides, sphingolipids in the absence or presence of water. *J. Mol. Biol.* 25:363–382.

Riske, K. A., and H. G. Dobereiner. 2003. Diacylglycerol-rich domain formation in giant stearoyl-oleoyl phosphatidylcholine vesicles driven by phospholipase C activity. *Biophys. J.* 85:2351–2362.

Ruiz-Argüello, M. B., G. Basañez, F. M. Goñi, and A. Alonso. 1996. Different effects of enzyme-generated ceramides and diacylglycerols in phospholipid membrane fusion and leakage. *J. Biol. Chem.* 271:26616–26621.

Ruiz-Argüello, M. B., F. M. Goñi, and A. Alonso. 1998. Vesicle membrane fusion induced by the concerted activities of sphingomyelinase and phospholipase C. *J. Biol. Chem.* 273:22977–22982.

Sillence, D. J., R. J. Raggers, and G. van Meer. 2000. Assays for transmembrane movement of sphingolipids. *Methods Enzymol.* 312:562–579.

Simon, C. G., and A. R. L. Gear. 1998. Membrane-destabilizing properties of C2-ceramide may be responsible for its ability to inhibit platelet aggregation. *Biochemistry.* 37:2059–2069.

Simons, K., and E. Ikonen. 2000. How cells handle cholesterol. *Science.* 290:1721–1726.

Siskind, L., and M. Colombini. 2000. The lipids C2- and C16-ceramide form large stable channels. Implications for apoptosis. *J. Biol. Chem.* 275:38640–38644.

Somerharju, P. 2002. Pyrene-labeled lipids as tools in membrane biophysics and cell biology. *Chem. Phys. Lipids.* 116:57–74.

Terrones, O., B. Antonsson, H. Yamaguchi, H. G. Wang, H. Liu, R. M. Lee, A. Herrmann, and G. Basoñez. 2004. Lipidic pore formation by the concerted action of proapoptotic BAX and tBID. *J. Biol. Chem.* 279:30081–30091.

Traikia, M., D. E. Warschawski, O. Lambert, J. L. Rigaud, and P. F. Devaux. 2002. Asymmetrical membranes and surface tension. *Biophys. J.* 83:1443–1454.

Veiga, M. P., J. L. R. Arrondo, F. M. Goñi, and A. Alonso. 1999. Ceramides in phospholipid membranes: effects on bilayer stability and transition to nonlamellar phases. *Biophys. J.* 76:342–350.

Zhou, Q., J. Zhao, J. G. Stout, R. A. Luhm, T. Wiedmer, and P. J. Sims. 1997. Molecular cloning of human plasma membrane phospholipid scramblase. A protein mediating transbilayer movement of plasma membrane phospholipids. *J. Biol. Chem.* 272:18240–18244.